Novel concepts for GaAs/LiNbO/sub 3/ layered systems and their device applications

M. Rotter, W. Ruile, G. Scholl, Achim Wixforth

Angaben zur Veröffentlichung / Publication details:

Rotter, M., W. Ruile, G. Scholl, and Achim Wixforth. 2000. "Novel concepts for GaAs/LiNbO/sub 3/ layered systems and their device applications." *IEEE Transactions on Ultrasonics, Ferroelectrics and Frequency Control* 47 (1): 242–48. https://doi.org/10.1109/58.818767.

Novel Concepts for GaAs/$LiNbO_3$ Layered Systems and Their Device Applications

Markus Rotter, Werner Ruile, Gerd Scholl, and Achim Wixforth

Abstract—**Thin semiconductor quantum well structures fused onto $LiNbO_3$ substrates using the epitaxial lift-off (ELO) technology offer the possibility of controlling the surface acoustic wave (SAW) velocity via field effect. The tunability of the conductivity in the InGaAs quantum well results in a great change in SAW velocity, in general, accompanied by an attenuation. We show that an additional lateral modulation of the sheet conductivity reduces the SAW attenuation significantly, enhancing device performance. At high SAW intensity, the bunching of electrons in the SAW potential also leads to a strong reduction of attenuation. These effects open new possibilities for voltage-controlled SAW devices. We demonstrate a novel, wireless, passive voltage sensor, which can be read out from a remote location.**

I. GaAs/$LiNbO_3$-Hybrids

The propagation velocity of SAW is strongly affected by the electrical boundary condition on the surface of the piezoelectric material. In conventional SAW devices, the surface impedance is fixed by the design and usually cannot be tuned externally. The combination of a piezoelectric material with the voltage-tunable surface impedance of a semiconductor device, however, allows for continuous change of the velocity. A great change in SAW velocity can be achieved on a material with a large electromechanical coupling coefficient K^2, e.g., $LiNbO_3$. We demonstrated a quasi-monolithic combination of $LiNbO_3$ and a GaAs quantum well structure for controlling the SAW velocity [1], [2].

This combination is achieved using the ELO, which was developed by Yablonovitch *et al.* [3]. The first use of this hybridization technique for SAW devices has been reported by Hohkawa *et al.* [4]. To fabricate the hybrids, a semiconductor-layered system is grown by molecular beam epitaxy, starting with an AlAs sacrificial layer on top of the GaAs substrate. This layer is followed by a modulation doped $In_{0.2}Ga_{0.8}As$ quantum well structure containing a two-dimensional electron system (2DES) (see Fig. 1). After covering the semiconductor structure with a black wax called Apiezon W, the AlAs layer is etched selectively in hydrofluoric acid. Then, the active layer system containing the 2DES is removed from the substrate and transferred onto the $LiNbO_3$ chip (128° rotation Y-cut, X-prop.) with the SAW transducer structure. The ELO film is tightly fixed only by van der Waals' forces. After this ELO process, the semiconductor film, which has a thickness of 0.5 μm, is patterned as shown in Fig. 1. Typical values for carrier concentration and room temperature mobility are $n_s = 5 \times 10^{11}$ cm^{-2} and $\mu = 4000$ cm^2/Vs. Because the 2DES is very close to the $LiNbO_3$ surface (the distance is only 32 nm), the conductivity of the electron system strongly influences the SAW propagation velocity v.

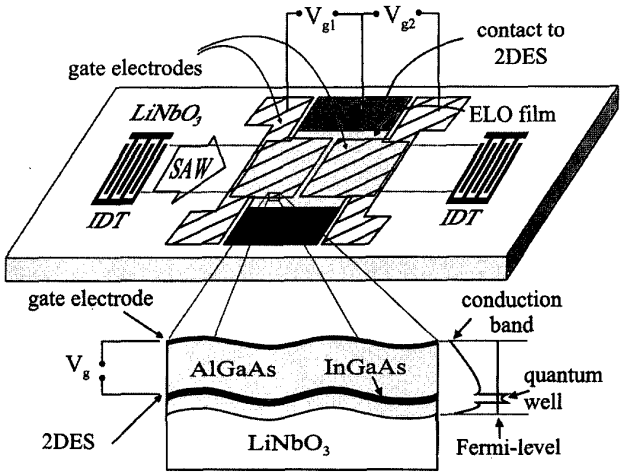

Fig. 1. Schematic sketch of the hybrid device (not drawn to scale) with two gates on top of the ELO film. The thickness of the ELO film is 0.5 μm, and the distance between $LiNbO_3$ and 2DES is just 32 nm. An RF signal is applied to one IDT to generate SAW. The lower part of the figure shows a schematic cross-section revealing the layer configuration and the energy of the conduction band in the semiconductor with respect to the Fermi level.

II. Attenuation and Velocity Change in the Hybrid

The interaction of the SAW and the 2DES results in a change of SAW phase velocity v and an attenuation Γ of the transmitted SAW intensity $I = I_0 \exp(-\Gamma l)$, where I_0 denotes the intensity of the SAW just entering the ELO film, and l is the length of the ELO film in the direction of SAW propagation [5], [6]. For our hybrid system, the sheet

Manuscript received June 15, 1999; accepted September 16, 1999.

M. Rotter and A. Wixforth are with Sektion Physik der LMU and CeNS, Geschw.-Scholl-Platz. 1, D-80539 München, Germany (e-mail: achim.wixforth@physik.uni-muenchen.de).

W. Ruile and G. Scholl are with Siemens AG, Corporate Technology, D-81730 München, Germany.

conductivity σ of the 2DES influences Γ and v as follows:

$$\Gamma = K_H^2 \frac{\pi}{\lambda} \frac{\sigma/\sigma_m}{1+(\sigma/\sigma_m)^2}$$
$$\frac{v - v_{sc}}{v_{oc}} = \frac{\Delta v}{v_{oc}} = K_H^2 \frac{1}{2} \frac{1}{1+(\sigma/\sigma_m)^2} \quad (1)$$

where λ is the SAW wavelength in the hybrid, v_{sc} denotes the hybrid velocity for the highly conductive electron system, and v_{oc} denotes the hybrid velocity for a depleted electron system. K_H^2 is the effective hybrid coupling coefficient, which is smaller than K^2 of $LiNbO_3$ because the gate electrode on top of the ELO film causes the velocity for a depleted electron system to be smaller than the velocity for a free $LiNbO_3$ surface. For a frequency of $f = 340$ MHz and $f = 434$ MHz and the described layered structure, the hybrid coupling coefficient is $K_H^2 = 3.3\%$ and $K_H^2 = 3.8\%$, respectively [2]. The coefficient σ_m denotes the conductivity at which maximum attenuation occurs and is approximately given by $\sigma_m = v\varepsilon_0 \left(\varepsilon_s \coth(2\pi h/\lambda) + \sqrt{\varepsilon_{11}^T \varepsilon_{33}^T - \varepsilon_{13}^T \varepsilon_{31}^T}\right) = 3.6 \times 10^{-6}\Omega^{-1}$ for a frequency of $f = 340$ MHz. ε_{ij}^T is the dielectric constant of $LiNbO_3$ under constant stress conditions, ε_s is the dielectric constant of the semiconductor film, and h is the distance between the gate electrode and the 2DES. If a voltage is applied to the gate electrode, the quantum well is depleted via field effect, resulting in a reduction of the sheet conductivity σ. This leads to an increase in SAW velocity.

If the gate voltage is applied homogeneously across the whole area of the ELO film, the change in SAW velocity is accompanied by a relatively large attenuation according to (1), which can be observed in Fig. 2 (see traces $'V_{g1} = V_{g2} = V_g'$; dashed lines). The insertion attenuation at $V_g = 0$ can be attributed to the bare SAW chip and the mechanical attenuation caused by the ELO film [2]. The attenuation maximum at $\sigma = \sigma_m$ limits device performance in the corresponding range of the gate bias. To overcome this drawback, we developed new concepts for the reduction of this attenuation.

III. Multiple Gate Structures

In principle, the idea is to distribute the attenuation over the whole range of gate bias, reducing the maximum attenuation. This can be achieved by dividing the ELO film into separated areas at different gate potentials and, correspondingly, different sheet conductivities. Fig. 1 shows the geometry of a hybrid device with two gate electrodes on top of the ELO film. The experimental results for this geometry are displayed in Fig. 2. If the gate voltage is applied to only one gate, with zero bias on the other, a phase shift and an attenuation of the transmitted RF signal can be observed (traces gate 1 and gate 2 in Fig. 2). Both gates show similar behavior. If the same gate voltage is applied to both gates at same time, attenuation and phase shift are added, resulting in a large phase shift and a nearly doubled attenuation at $V_g = -7.7V$ (dashed traces; $'V_{g1} = V_{g2} = V_g'$).

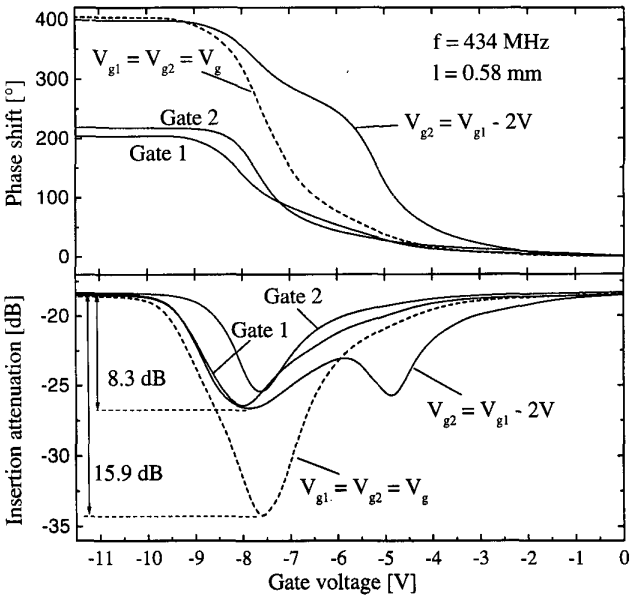

Fig. 2. Insertion attenuation and phase shift of the transmitted signal in a hybrid with two gates on top of the ELO film (according to Fig. 1) for different gate bias configurations. The traces labeled by Gate 1 and Gate 2 display the phase shift and attenuation of the device with only one gate swept (namely Gate 1 or Gate 2); the corresponding gate is grounded. The quantity l denotes the length of that part of the ELO film, which is covered by gate electrodes. All measurements are at room temperature.

This maximum attenuation can be reduced significantly when different voltages are applied to the gates. In Fig. 2, we show a particular measurement at which an additional offset bias of -2 V was applied to gate 2 (see traces $'V_{g2} = V_{g1} - 2V'$). This results in a shift of the attenuation and phase curves of gate 2. The total phase shift is the same as that for identical voltages. However, the total attenuation is much smaller when a gate voltage offset is applied because the overall attenuation is distributed over two different regions of the gate voltage.

A further reduction of insertion loss can be achieved by fabricating more than two gates on top of the ELO film. In Fig. 3, a hybrid with four gates is presented. The SAW characteristics of the four single gates were measured and are displayed in Fig. 3. Apart from slightly different threshold voltages, which can be explained by the fabrication process, all four gates show the expected behavior.

When the same gate voltage is applied to all gates, the phase shifts and attenuation curves are superposed. Because of the small offsets of the single gate traces, the total attenuation is slightly less than the sum of the maximum attenuation of the single gates. Further, the total attenuation can be distributed across a wider gate voltage range by applying different gate voltages. Here, gate bias offsets of 1, 2, and 3 V were applied to the respective gate. This reduced the total electronical attenuation by 15 dB, from -23.4 to -8.4 dB. In this multiple-gate device, the

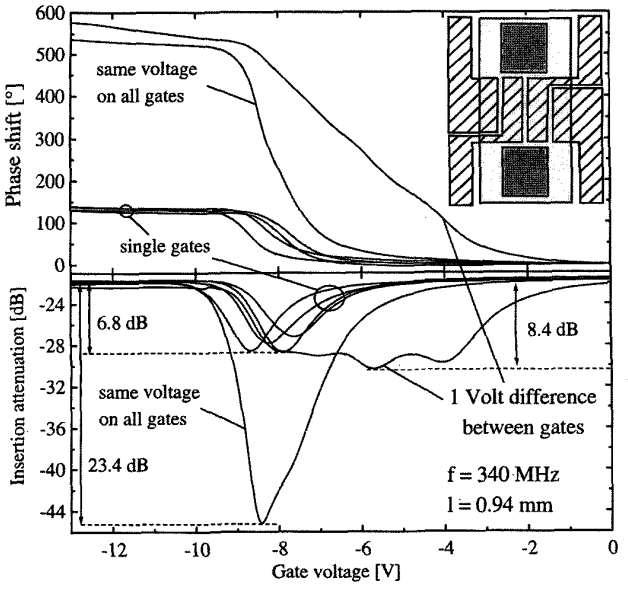

Fig. 3. Attenuation and phase shift in a device with four separated gate electrodes. The inset displays the geometry of the semiconductor structure. The ELO film is light gray, the Ohmic contacts are dark gray, and the gates are hatched.

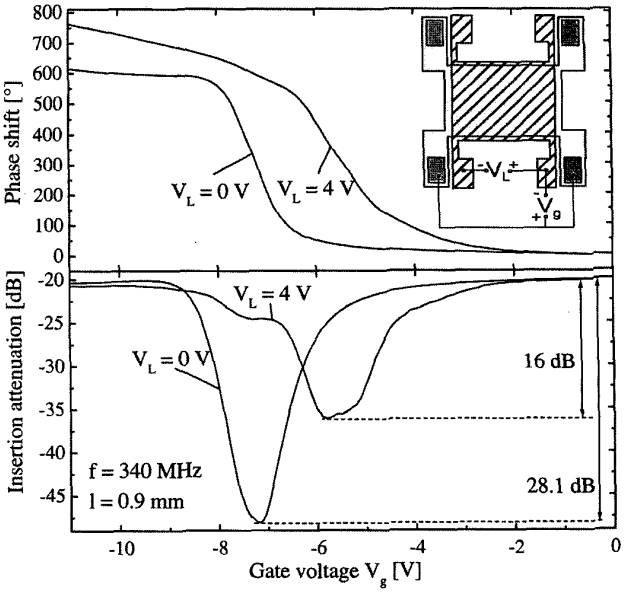

Fig. 4. Phase shift and corresponding insertion attenuation in a device with resistive (Ohmic) gate electrode. A longitudinal voltage V_L results in enhancement of SAW transmission.

phase shift is very close to a linear function of the gate voltage, which is very useful for most applications when a simple linear relationship between voltage and phase shift is desired. If a larger voltage offset is applied between the gates, the overall attenuation could be minimized further to a value of 6.8 dB, but this would cause steps in the phase shift curve and, therefore, would reduce the linearity of the phase shift.

Comparing the devices with two and four gates, it is evident that the maximum electronic attenuation in the four-gate geometry is smaller than that with just two gates. In addition, the phase shift as a function of gate voltage is more linear in the four-gate device. On the other hand, it is more complicated to apply four different gate voltages. This could be managed with an on-chip resistive voltage divider circuit, which yields similar results as a constant voltage shift between the gates.

IV. Continuous Potential Gradient

When the number of gate electrodes is increased, the potential drop between the electrodes becomes smaller. For a very large number, the channel potential becomes a continuous, linear function of the position in the channel. As the electron system produces significant attenuation only in the region at which $\sigma = \sigma_m$, only a small area of the ELO film would contribute to the overall attenuation. Therefore, we would expect a large reduction of attenuation in a geometry with a linear potential gradient in the channel along the SAW propagation path.

Such a potential gradient in the channel can be realized, for example, by producing a longitudinal voltage drop along a highly resistive gate electrode on top of the ELO film in the direction of SAW propagation, as displayed in the inset of Fig. 4. We realized this structure with a thin Ni/Cr gate electrode (thickness, 5 nm). In Fig. 4, we show the results of insertion loss and phase shift. If a longitudinal voltage V_L is applied, we achieve a continuous change of the local field effect potential and, therefore, also a conductivity gradient along the propagation direction. Furthermore, this distributes the total attenuation over a larger range of gate bias and, therefore, reduces the maximum of SAW attenuation caused by the 2DES. In this first simple device, a larger voltage drop across the gate electrode leads to high currents in the gate. However, the power consumption of the gate could be reduced significantly by employing a meander-shaped gate electrode with a much larger total resistance.

V. Reduction of Attenuation Caused by Electron Bunching

Up to now, we made the assumption that the modulation of the carrier density by the SAW is only small compared with the total carrier concentration. In this case, (1) can be employed to describe the behavior of attenuation and velocity change. However, for high SAW intensity, this model fails because the electron density modulation becomes large. The experiment shows that, in this case, the attenuation is strongly reduced with an increase of SAW amplitude (Fig. 5). At small SAW intensities, the electronic attenuation is 4.5 dB for this sample; for high wave intensities (RF level $P = 19$ dBm) corresponding to an effective SAW potential amplitude of $\Phi_0 = 0.92$ V,

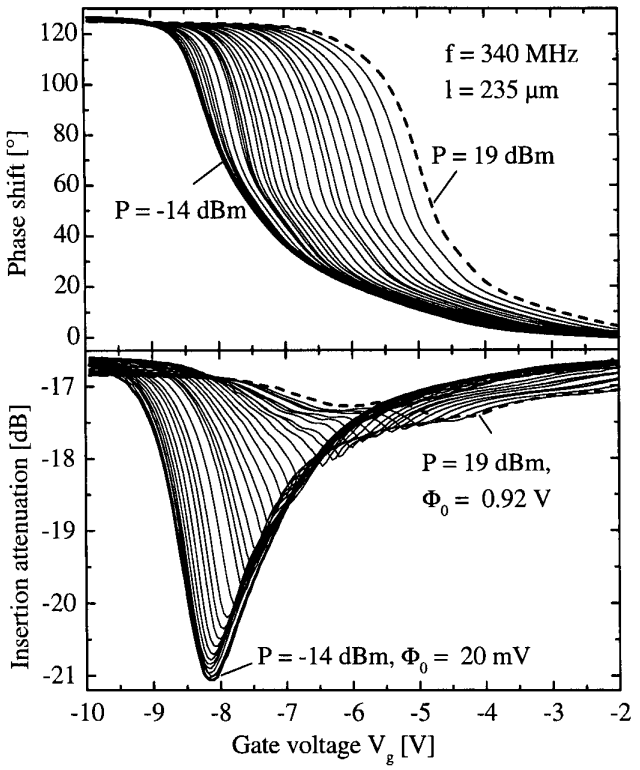

Fig. 5. Attenuation and phase shift as a function of gate bias for different RF powers. For increasing SAW intensity, the electronic attenuation is strongly reduced because of the bunching of the electrons. The total phase shift remains constant. In this experiment, a geometry with only one gate and a single gate bias V_g is used.

the attenuation is reduced to only 0.8 dB. To explain this behavior, we developed a new nonlinear theory [7]; we calculate the local electron density in the wave potential and the local current density j induced by the SAW field E_{SAW}. For high SAW intensity I and small carrier density n_s, the electrons are completely trapped in the SAW potential. Then, the electrons are forming stripes moving at the speed of sound. This phenomenon is known as acoustic charge transport [8]–[10]. The absorbed SAW energy is given as $Q = I\Gamma = \langle jE_{\mathrm{SAW}} \rangle$, where brackets denote the average over one SAW period. Numerical calculations show that the absorbed energy Q saturates with increasing SAW intensity I, and, therefore, the attenuation Γ is reduced [7]. This can also be explained in terms of the average drift velocity of the electrons in the SAW potential. When I is increased, the drift velocity is also increased, eventually saturating at the SAW velocity, where the electrons are captured in the valleys of the wave potential. The model is also in good quantitative agreement with the experiment [7] and even reproduces the shift of the maximum attenuation toward higher conductivity (see Fig. 6).

The total velocity change, however, remains constant when the SAW intensity changes. The curves only shift slightly toward higher conductivity when increasing the SAW potential, in analog to the attenuation. It can be understood easily, that the total velocity change is not affected by the SAW amplitude. For a highly conductive 2DES ($V_g = 0$), the SAW potential is strongly screened by the electrons, despite the high potential amplitude, resulting in the velocity for the short circuit case. Decreasing the conductivity, the modulation of the 2DES becomes stronger, leading to a bunching of electrons in the valleys of the potential. Starting at a fully conductive electron sheet in the quantum well for $V_g = 0$, the area of high conductivity is reduced with decreasing electron density because of the forming of conductivity stripes. For a totally depleted quantum well, even the valleys of the SAW potential are empty, and the SAW velocity is equal to the velocity for zero conductivity and low SAW intensity.

The effect of reduced SAW attenuation is very promising for new voltage-tunable devices with good performance even at $\sigma = \sigma_m$. Fig. 6 shows that the attenuation is nearly vanishing at $P = 19$ dBm. This relatively high RF power level can be reduced significantly by optimizing the design of the SAW device. For the first experiments described here, the interdigital transducers (IDT) were optimized for operation on four different harmonic frequencies, resulting in an insertion loss for the unmatched bare $LiNbO_3$ SAW device of 12.5 dB. Employing impedance-matched, single-phase, unidirection transducers (SPUDTs), the insertion loss could be reduced by about 9.5 dB. A reduction of the IDT aperture from presently 600 μm to 300 μm would also double the SAW intensity. Such an optimized device could produce an effective SAW potential amplitude of 0.9 V by applying an RF power of only 11.5 dBm, which is in the range of operation power for standard SAW devices.

The nonlinear behavior of the attenuation as a function of SAW intensity can also be used to develop novel, passive, nonreciprocal SAW devices. If two different IDT designs are employed to generate acoustic waves with different efficiencies, a certain RF power level would lead to different SAW intensities when applied to the IDTs. For example, a SPUDT with small aperture on the one side of the ELO film would produce a much higher SAW intensity than a bidirectional IDT with large aperture on the other side of the device. Operated at $\sigma = \sigma_m$, the SAW device is nonreciprocal, $S_{21} \neq S_{12}$. Because a quantum well structure could be designed to satisfy $\sigma = \sigma_m$ at $V_g = 0$, this effect offers the possibility for a passive, nonreciprocal SAW device.

VI. Application of the Hybrid as a Remote Voltage Sensor

The hybrid technology is very interesting for new SAW devices. The most evident application is a voltage-controlled SAW delay line, i.e., the delay time of an RF signal is tuned by the applied gate bias. Also, a voltage-controlled oscillator is feasible [2]. An ELO film is combined with a SAW delay line oscillator to change the phase in the oscillator loop. Here, we would like to demonstrate the applications of the hybrid system as a novel remote voltage sensor. Passive remote sensing of a large variety of

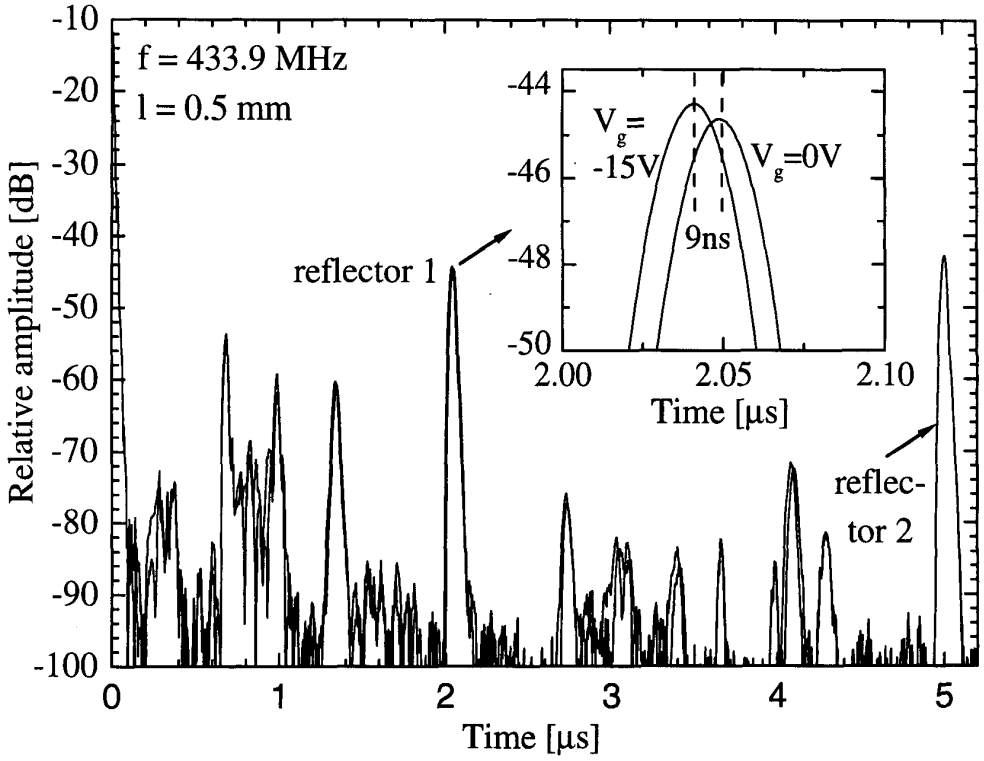

Fig. 6. Signal response of the voltage sensor as a function of time for $V_g = -15$ V and $V_g = 0$ V. The reflector structures produce response signals at $t = 2$ μs and $t = 5$ μs. The inset shows an enlargement of the response signal from reflector 1 in order to display the change in delay time of the signal for different gate bias.

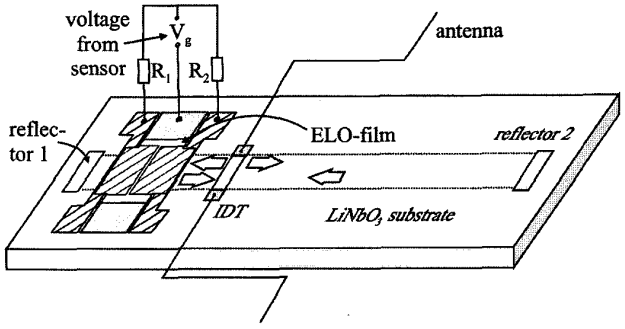

Fig. 7. Schematic geometry of a remote voltage sensor. An antenna attached to the IDT allows for the conversion of a radio pulse into SAW and vice versa.

physical quantities as temperature [11], [12], [13], torque [13], and pressure [14] has recently attracted much interest. The operation principle is shown in Fig. 7. On the $LiNbO_3$ chip, one IDT and two reflector structures are fabricated. An antenna is attached to the IDT. An interrogating pulse that is sent to the device from a remote location is converted by antenna and IDT into a SAW pulse, propagating on the $LiNbO_3$ chip in both directions toward the reflectors. The waves are reflected at the reflector structure, and the returning SAW are converted back into an RF signal emitted by the antenna. An interrogation unit measures the phase relationship between the two reflected pulses. Because of the long delay time of the interrogating signal, all environmental echoes of the signal have dissipated by the time the signal has returned to the interrogation unit, and the signal can be analyzed without interference. In one acoustic beam path, the ELO film is placed, transforming an applied sensor voltage V_g into a change of SAW velocity. Fig. 6 shows the measured relative amplitude of the reflected signal as a function of time. $t = 0$ corresponds to the time of the interrogation pulse. At $t = 2$ μs, the signal from reflector 1 can be detected; at $t = 5$ μs, the second signal (reflector 2) is measured, which is only used as a reference signal. The change in gate bias produces a change in the signal group delay time of 9 ns for an ELO film length of 0.5 mm, as depicted in the inset of Fig. 6. Because the SAW traverses the region of the ELO film twice, the phase shift and the group delay time change of the signal is twice as large as in the previously discussed geometry (Fig. 1).

Fig. 8 displays the phase shift and the absolute attenuation of the reflected signal with respect to the interrogation signal as a function of the gate bias. In this device, a geometry with two gate electrodes was chosen. To achieve a voltage difference between the two gates to reduce the electronic attenuation, two on-chip resistors with different very high ohmic resistance fabricated by a thin NiCr connection evaporated on the chip were employed. These

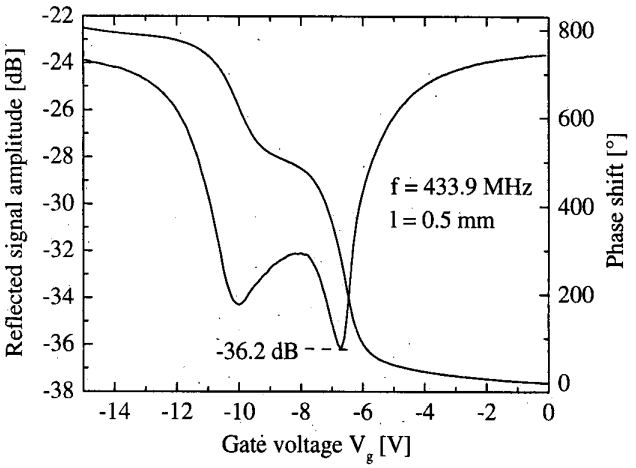

Fig. 8. Absolute reflected signal amplitude of reflector 1 as a function of gate bias V_g. Also shown is the phase shift of the signal with respect to reflector 2. This phase shift is the quantity that is used to extract the applied sensor voltage V_g.

series resistors R_1 and R_2 (Fig. 7) produce a voltage offset between the gate electrodes. This results in a strongly reduced total attenuation following the same principle as in Fig. 2.

If any sensor that produces a voltage in the range displayed in Fig. 8, e.g., a solar cell or a piezoelectric sensor, is attached to the hybrid device, then its sensor voltage can be read out from a remote location by an interrogating RF pulse. No additional power supply is needed for the sensor. Because the leakage current through the gate is very small, the hybrid SAW sensor is nearly free of power consumption.

VII. Conclusions

The voltage-controlled sheet conductivity of a semiconductor film on a $LiNbO_3$ SAW device can be employed for tuning the SAW velocity. However, at a certain conductivity σ_m, energy is dissipated by the electron system, reducing device performance at the corresponding gate bias. We demonstrate new device geometries that enhance SAW transmission significantly by a spatially inhomogenous conductivity distribution. Multiple gate structures distribute the SAW attenuation over a wide range of gate bias and, therefore, reduce the maximum of attenuation presently from -23.4 to -8.4 dB. Because of the field effect, these devices are nearly free of power consumption. Alternatively, a linear potential gradient along the gate electrode can be employed for the distribution of attenuation. At high SAW intensities, the attenuation caused by the electrons is also reduced because of the bunching of the electrons in the valleys of the SAW potential. This nonlinear effect can be also employed to design nonreciprocal, passive SAW devices.

These strongly improved SAW transmission parameters allow for various SAW device applications. Here, we demonstrate a remote SAW voltage-sensing device. A nearly arbitrary sensor producing an output voltage can be attached to this hybrid layered system, so that the sensor voltage can be read out wireless from a remote location.

Acknowledgment

We thank S. Manus, T. Ostertag, W. Gawlik, and S. Berek for technical assistance and D. Bernklau and H. Riechert for the growth of excellent MBE structures. We gratefully acknowledge fruitful discussions with J. P. Kotthaus, A. O. Govorov, and C. Ruppel.

References

[1] M. Rotter, C. Rocke, S. Böhm, A. Lorke, A. Wixforth, W. Ruile, and L. Korte, "Single-chip fused hybrids for acousto-electric and acousto-optic applications," *Appl. Phys. Lett.*, vol. 70, pp. 2097–2099, Apr. 1997.

[2] M. Rotter, W. Ruile, A. Wixforth, and J. P. Kotthaus, "Voltage controlled SAW velocity in GaAs/$LiNbO_3$-hybrids," *IEEE Trans. Ultrason., Ferroelect., Freq. Contr.*, vol. 46, pp. 120–125, Jan. 1999.

[3] E. Yablonovich, D. M. Hwang, T. J. Gmitter, L. T. Florez, and J. P. Harbison, "Van der Waals bonding of GaAs epitaxial liftoff film onto arbitrary substrates," *Appl. Phys. Lett.*, vol. 56, pp. 2419–2421, Jun. 1990.

[4] K. Hohkawa, H. Suzuki, Q. S. Huang, and S. Noge, "Fabrication of surface acoustic wave semiconductor coupled devices using epitaxial lift-off technology," in *Proc. IEEE Ultrason. Symp. 1995*, pp. 401–404, 1995.

[5] K. A. Ingebrigtsen, "Linear and nonlinear attenuation of acoustic surface waves in a piezoelectric coated with a semiconductor film," *J. Appl. Phys.*, vol. 41, pp. 454–459, Feb. 1970.

[6] A. Wixforth, J. P. Kotthaus, and G. Weimann, "Surface acoustic waves on GaAs/$Al_xG_{1-x}As$ heterostructures," *Phys. Rev.*, vol. B40, pp. 7874–7886, Oct. 1989.

[7] M. Rotter, A. V. Kalameitsev, A. O. Govorov, W. Ruile, and A. Wixforth, "Charge conveyance and nonlinear acoustoelectric phenomena for intense surface acoustic waves on a semiconductor quantum well," *Phys. Rev. Lett.*, vol. 82, pp. 2171–2174, Mar. 1999.

[8] M. J. Hoskins, H. Morkoç, and B. J. Hunsinger, "Charge transport by surface acoustic waves in GaAs," *Appl. Phys. Lett.*, vol. 41, pp. 332–334, Aug. 1982.

[9] W. J. Tanski, S. W. Merritt, R. N. Sacks, D. E. Cullen, E. J. Branciforte, R. D. Caroll, and T. C. Eschrich, "Heterojunction acoustic charge transport devices on GaAs," *Appl. Phys. Lett.*, vol. 52, pp. 18–20, Jan. 1988.

[10] R. N. Sacks, W. J. Tanski, S. W. Merritt, D. E. Cullen, E. J. Branciforte, and T. C. Eschrich, "Acoustic charge transport in an (Al,Ga)As/GaAs heterojunction structure grown by MBE," *J. Vac. Sci. Technol. B*, vol. 6, pp. 685–687, Mar./Apr. 1988.

[11] X. Q. Bao, W. Burghard, V. V. Varadan, and K. V. Varadan, "SAW temperature sensor and remote reading system," *Proc. IEEE Ultrason. Symp.*, 1987, pp. 583–585.

[12] F. Seifert, W.-E. Bulst, and C. Ruppel, "Mechanical sensors based on surface acoustic waves," *Sens. Actuators*, vol. A44, pp. 231–239, 1994.

[13] L. Reindl, G. Scholl, T. Ostertag, H. Scherr, U. Wolff, and F. Schmidt, "Theory and application of passive SAW radio transponders as sensors," *IEEE Trans. Ultrason., Ferroelect., Freq. Contr.*, vol. 45, pp. 1281–1292, Sep. 1998.

[14] H. Scherr, G. Scholl, F. Seifert, and R. Weigl, "Quartz pressure sensor based on SAW reflective delay line," *Proc. IEEE Ultrason. Symp.*, 1996, pp. 347–350.

Markus Rotter was born in 1971 in Munich, Germany. He received the diploma in physics degree in 1996 and the Dr. rer. nat. degree in physics in 1999 from the Ludwig-Maximilians-University in Munich. Since his diploma thesis, he is engaged in a cooperation between the University of Munich and the Siemens Laboratories in Munich, focusing on device applications for the acoustoelectric interaction between SAW and a 2DES.

Werner Ruile was born in Augsburg, Germany, in 1955. He received the diploma in physics degree from the Ludwig-Maximilians-University, Munich, Germany, in 1983. From the Institute of High Frequency Engineering at the Technical University of Munich, he received his Dr. Ing. degree in 1993. Since 1983, he has been with the microacoustic group of the Siemens Research Laboratories Munich, where he is involved in research and modeling of SAW devices.

Gerd Scholl was born in Aalen, Germany, in 1963. In 1989, he received the Dipl. Ing. degree and, in 1997, the Dr. Ing. degree, both in electrical engineering, from the Technical University of Munich, Germany. He has been with the microacoustics group of the Siemens Corporate Technology department, Munich, Germany, where he is engaged in the research and development of SAW low-loss filters and wireless sensor systems, since 1989.

Achim Wixforth was born in Bielefeld, Germany, in 1956. He received the diploma in physics degree from the University of Hamburg in 1984 for low temperature investigations of minigaps on high index surfaces on semiconductor MOS systems. In 1987, he received his Dr. rer. nat. degree in physics for his exploratory and pioneering work on the interaction between SAW and low-dimensional electron systems in semiconductor nanostructures. As an assistant research engineer, he spent 1989 at the University of California, Santa Barbara, where he focused on molecular beam epitaxy of graded bandgap semiconductors. In 1990, he went into far-infrared spectroscopy of bandgap engineered materials, concentrating on plasmon, cyclotron resonance, and intersubband resonance phenomena. In 1994, he finished his habilitation and received the Dr. rer. nat. habil. degree in experimental physics from the Ludwig-Maximilians-University of Munich. Since then, he has worked in Munich as university lecturer. His research interests include collective phenomena, transport, optical, and SAW studies of low dimensional semiconductors.

In 1992, Dr. Wixforth received a Fellowship Award for significant contributions to the physics of phonons, sponsored by the IBM Corporation, Japan. In 1998, he was awarded the Walter Schottky prize for solid state physics.